Int. J. Electrochem. Sci., 14 **(2019)** 11300 – 11311, doi: 10.20964/2019.12.73

International Journal of
ELECTROCHEMICAL
SCIENCE
www.electrochemsci.org

Short Communication

Corrosion Behavior of Printed Circuit Boards in Tropical Marine Atmosphere

Yali Feng[1,2], Ziheng Bai[1,2], Qiong Yao[3], Dongjiu Zhang[3], Jialiang Song[1,2],Chaofang Dong[1,2], Junsheng Wu[1,2], Kui Xiao[1,2,]*

[1] Corrosion and Protection Center, Institute of Advanced Materials and Technology, University of Science and Technology Beijing, Beijing 100083, China.
[2] National Materials Corrosion and Protection Data Center, University of Science and Technology Beijing, Beijing 100083, China.
[3] Key Laboratory of Space Launching Site Reliability Technology, Haikou 571000, China.
[*]E-mail: xiaokui@ustb.edu.cn

Received: 25 June 2019 / *Accepted:* 7 September 2019 / *Published:* 29 October 2019

Outdoor exposure experiments of PCB-Cu, PCB-ImAg and PCB-ENIG were conducted in a tropical marine atmosphere under the synergistic effect of multiple factors, and the corresponding corrosion behavior of the PCBs was investigated by SEM, EDS and EIS. The results indicated that PCB-ImAg had strong resistance to Cl^-, and the surface was covered only by several spores, without obvious corrosion products, and it had excellent corrosion resistance. PCB-ENIG was covered with dense corrosion products, and it had poor biocompatibility and was detrimental to the growth of molds. PCB-Cu was significantly corroded, and an obvious shedding of surface corrosion products was observed, with the corrosion rate increasing constantly during the exposure periods. All the corrosion occurred at the active sites where dust particles, salt particles and mold spores were scattered. The probable corrosion mechanism of PCBs inferred that defects in the coatings of PCB-ImAg and PCB-ENIG acted as pathways for the corrosive electrolyte liquid, and the copper substrate was corroded, and localized corrosion cells accelerated the corrosion. Additionally, long-term exposure led to the formation of a double-layer structure in PCB-Cu, with an inner oxide film and an outer layer of loose corrosion products, consequently providing a weak protection effect.

Keywords: Corrosion; PCB; Tropical marine atmospheric environment; Exposure experiments.

1. INTRODUCTION

With the rapid development of electronics and related industries, printed circuit boards (PCBs) have become widely used in various electronic devices. The extensive application and increasing requirements of PCBs have promoted development towards miniaturization and integration, leading to

their greater electrochemical instability and sensitivity to external factors [1], which means that even a small amount of corrosion products can significantly affect the reliability of electronic devices [2]. As a result, the corrosion problem of PCBs is receiving increasing attention. As the demand for marine resources has increased quickly, the exploration and exploitation of marine resources are gaining increased attention, thus promoting extensive applications of electronic devices. However, the severe marine atmosphere environment of high chloride concentration, high humidity and abundant microorganisms markedly increases the corrosion tendency of PCBs. Thus, the corrosion problem of PCBs in marine atmosphere environments is a significant matter.

Because of the important properties, such as excellent electrical and thermal conductivity, reliability of solder joints and affordability, copper and its alloys are often used as substrate materials for PCBs [3-5]. However, a copper-clad plate (PCB-Cu) is prone to suffer from surface oxidation and corrosion [6, 7], so certain surface treatments, including electroless nickel immersion gold (ENIG), immersion silver (ImAg), hot air solder leveling (HASL) and organic solderability preservative (OSP) technologies are applied to the PCB-Cu surface to improve the corrosion resistance of PCBs [8, 9]. These surface treatments can significantly inhibit the corrosion of PCBs because of the protective layers, but the corrosion of PCBs, especially microporous corrosion, can still occur [10-12].

Most PCBs are used in an atmospheric environment. In actual service conditions, the surfaces of PCBs are prone to be covered with a thin electrolyte layer produced by condensation or adsorption, containing aggressive substances such as deposited salt particles, dust particles and adsorbed mold spores, and changes in the thickness of the electrolyte layer can affect several corrosion-related processes, which can result in the electrochemical corrosion failure of PCBs [12, 13]. It has been reported that the corrosion process of PCBs is a synergistic effect of many environment factors, including temperature, humidity, contaminants (Cl^-, SO_4^{2-}, SO_2, H_2S, etc.), microorganisms and electric fields [14-20]. When PCBs are in service in a marine atmosphere environment, a large amount of salt particles are deposited on the surface of PCBs, and vapor condenses or adsorbs at these active sites preferentially to form an electrolyte layer, accelerating the atmospheric corrosion process of metals [21]. Additionally, the high relative humidity (RH) level of the marine atmosphere environment is more likely to promote the formation of a thin electrolyte layer, and an accelerated corrosion effect of increasing RH on the surface of PCBs has been observed [22]. In addition, the microbially influenced corrosion of PCBs cannot be neglected, especially in the high humidity of marine atmosphere environments, which tends to promote the growth of molds [23]. The corrosion effect from molds is one of the important factors affecting the reliability of PCBs, and it was found that the growth and metabolism of molds could promote the microporous corrosion of PCB-ImAg and PCB-ENIG [19, 20]. However, previous research on the corrosion of PCBs has mostly focused on the effect of only one of the environmental factors by indoor simulation experiments, which cannot simulate the actual corrosion failure process resulting from the synergistic effects of multiple factors in practical service. Only a few investigations have been conducted in outdoor atmosphere environments or industrially polluted marine atmosphere environment [4, 9, 11, 12]; there is little research on the corrosion of PCBs in tropical marine atmospheric environments with a high temperature at which corrosion is prone to occur.

To study the suitability and corrosion behavior of PCBs in a tropical marine atmosphere under the synergistic effects of high temperature, high humidity, high concentrations of Cl^- and abundant microorganisms, outdoor exposure experiments were conducted in Hainan Province, China, which is located in a tropical area of low latitude where the temperature is generally higher than that of other outdoor exposure places. After the outdoor exposure experiments, scanning electron microscopy (SEM), energy dispersive spectrometry (EDS) and electrochemical impedance spectroscopy (EIS) were utilized to investigate the corrosion behavior of PCBs treated by different surface technologies in the tropical marine atmosphere.

2. EXPERIMENTAL

2.1. Materials and experimental methods

PCB-Cu, PCB-ImAg and PCB-ENIG (Sprine Co., China) were used as the experimental samples. The basic parameters of the PCBs are listed in Table 1. As shown in Table 1, the board samples were 0.8 mm in thickness and made of FR-4 epoxy glass cloth laminate. The thickness of the copper substrate was 25-30 μm. The effective size of the samples was 20 mm × 3 mm, and the spacing between two identical neighboring samples was 0.5 mm. Before the experiments, the samples were sequentially washed with deionized water and alcohol for 5 minutes. Then, the samples were placed on a sterile operating table for ultraviolet sterilization.

Table 1. Basic parameters of PCBs.

Items	PCB-Cu	PCB- ImAg	PCB-ENIG
Board materials	FR-4	FR-4	FR-4
Board thickness (mm)	0.8	0.8	0.8
Copper substrate thickness (μm)	25-30	25-30	25-30
Surface treatments	/	silver immersion	gold immersion
Coating thickness (Ag or Au/Ni, μm)	0	0.02 / 0.1	0.05 / 0.1

All the samples were exposed in Hainan Province, China, for the outdoor exposure experiments. The PCB samples were placed in a cabinet with a shutter structure, which helped to keep samples from rain and to ensure ventilation during the outdoor exposure test. After 3 and 6 months (m), the samples were taken back to the laboratory for further analysis.

2.2. Surface analysis methods

After the outdoor exposure experiments, the morphology of surface corrosion was observed by scanning electron microscopy (SEM) (FEI Quanta 250 FEG). The compositions of corrosion products were detected by energy dispersive spectroscopy (EDS) (DEAX).

2.3. Electrochemical methods

Electrochemical measurements were conducted using a PAR2273 advanced electrochemical system from Princeton Applied Research. The electrochemical measurements were all based on a three-electrode system, where the sample was used as a working electrode (WE), and a platinum foil and a saturated calomel electrode (SCE) served as a counter electrode (CE) and reference electrode (RE), respectively. The electrochemical working area of the WE was 1.2 cm^2. The Luggin capillary of the SCE was positioned close to the WE surface in order to minimize ohmic potential drop.

Electrochemical impedance spectroscopy (EIS) measurements were carried out at the end of open circuit potential (OCP) with a frequency range from 100 kHz to 10 mHz. All experiments were performed in 0.1 mol/L Na_2SO_4 solution. The test temperature was maintained at 37°C during the entire test process by a thermostatically controlled water tank. Each experiment was repeated at least three times to ensure reproducibility. The EIS data were fitted using ZSimpWin software.

3. RESULTS AND DISCUSSION

3.1. SEM and EDS analysis

The SEM morphology of the PCB samples after 3 months of outdoor exposure is shown in Fig. 1. Additionally, EDS was collected from the particles in Fig. 1 (a-1), (b-1) and (c-1), and the EDS results are shown in Fig. 2. As the SEM images show, all the surfaces of PCB-Cu, PCB-ImAg and PCB-ENIG were covered with particles or corrosion products, but the corrosion morphology of the various surface-treated samples differed from each other.

It can be seen from Fig. 1a that severe corrosion occurred on the surface of PCB-Cu. Obvious shedding of surface layers was observed, with a large amount of spherical particles scattered on the PCB-Cu surface. In addition to the large spherical particles, small branched products were also observed on the PCB-Cu surface, accompanied by small particles around the distribution, as shown in the enlarged image in Fig. 1 (a-3). As the copper was prone to corrosion and the formed product layers were covering the PCB-Cu surface [6, 7], outdoor exposure would lead to the shedding of surface layers. The EDS analysis of the spherical particles in Fig. 2a shows the presence of C, O, Cu, Cl, Na, P and N. The presence of Cu confirmed the dissolution of the substrate copper. Since C, O, P and N are biological components of molds or their metabolites [19], it can be asserted that the spherical particles were mold spores. Additionally, salt particles (NaCl) were detected. When PCB-Cu samples were exposed in the marine atmosphere environment of Hainan, salt particles would deposit on the PCB-Cu surface, and the moisture absorption of salt particles aided the abundant water vapor in the air to form corrosive electrolyte layers, accompanied by the absorption, growth and metabolism of molds. All the activated sites where salt particles deposited and mold spores gathered would be unstable electrochemically, and localized corrosion would occur. Over time, corrosion products gradually accumulated.

As for PCB-ImAg, SEM images (Fig. 1b) show that there were some porous spherical particles scattered on its surface. The EDS results of the particles are shown in Fig. 2b. Due to the presence of the silver protective layer, a nickel buffer layer and the copper substrate, the elements Ag, Ni and Cu

were detected. The organic elements C, N and P were related to mold. In addition, the presence of Cl demonstrated the deposition of Cl^-, which had an accelerating effect on corrosion.

The SEM images of PCB-ENIG in Fig. 1c show that the surface of PCB-ENIG was apparently corroded. The surface was covered by dense corrosion products, and the accumulated corrosion products were significantly cracked. Once the product layer shed from the substrate, the inner materials would be exposed to the atmospheric environment directly, which would result in the corrosion of the substrate materials. Though it can be seen that the corrosion product layer cracked, no obvious shedding occurred. No spherical spores were observed, but organic elements C, N and P were detected in the EDS results of corrosion products in Fig. 2c, which indicated the protective layer of Au was detrimental to the attachment and growth of molds. It can be inferred that after 3 months of exposure, the immersion gold layer lead to the death of the microorganisms, and only the metabolites of the microorganisms remained.

In general, the corrosion of PCB-Cu without a protective layer was the most serious, followed by PCB-ENIG, while no obvious characteristics of corrosion were observed on PCB-ImAg, and only several spores were scattered on its surface, which differs from previous reports showing that the corrosion level of silver-plated circuit boards on computers serving in an industrial environment containing reduced sulfur gas was higher than that of gold-plated circuit boards [24]. The different corrosion resistance performances of circuit boards immersed by silver and gold under the tropical marine atmosphere and industrial environment seemed to be related do the sensitivity of the protective metal to the corrosive substances in the environment. Additionally, the biocompatibility of PCB-ENIG was poor and was probably detrimental to the growth of molds. Further, the observed corrosion of PCBs generally occurred at activated sites where salt particles deposited or spores absorbed.

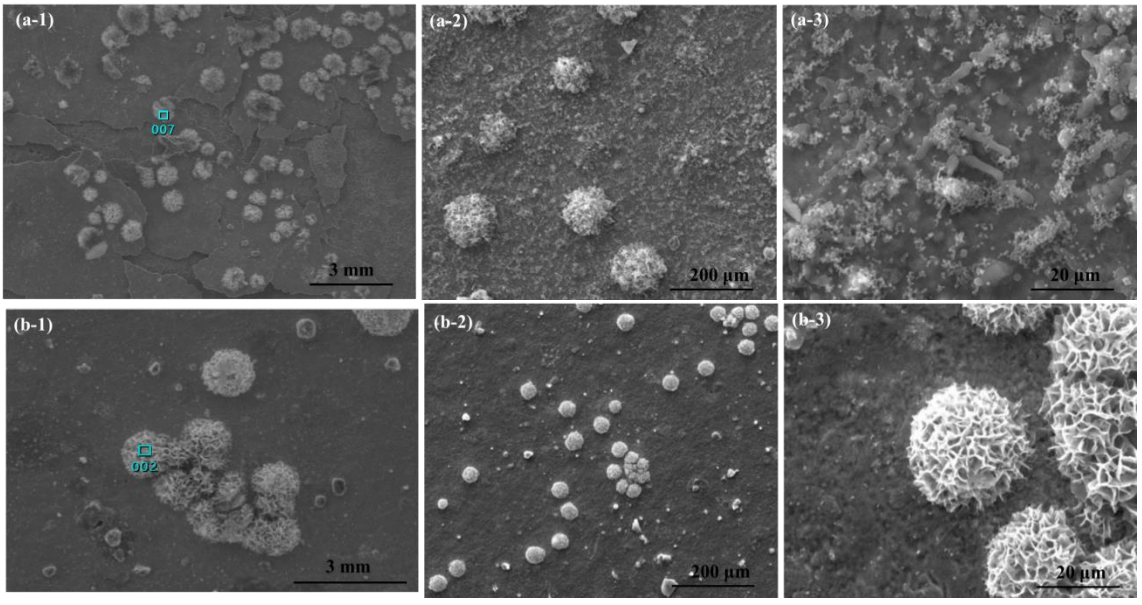

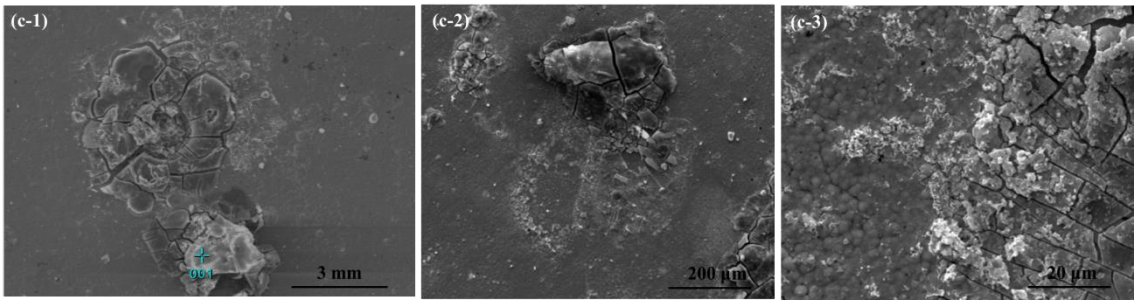

Figure 1. SEM morphology of (a) PCB-Cu, (b) PCB-ImAg, (c) PCB-ENIG exposed outdoors for 3 months at different amplification ratios.

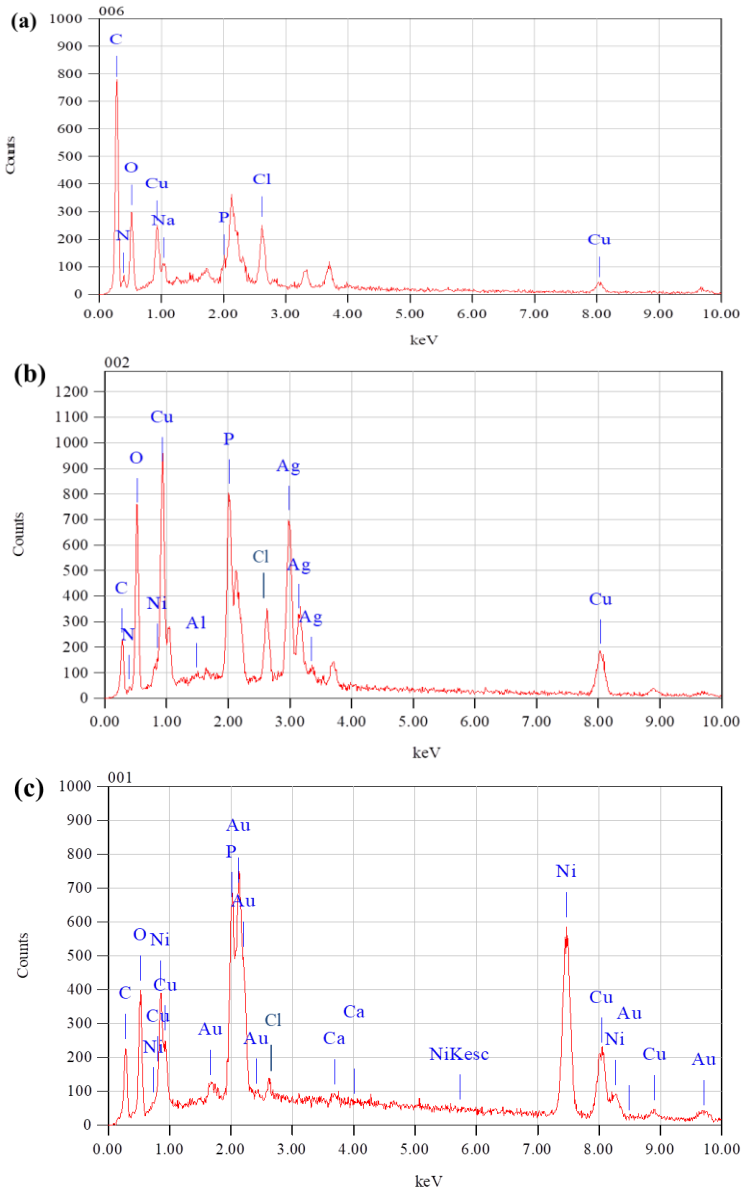

Figure 2. EDS results of (a) PCB-Cu, (b) PCB-ImAg, (c) PCB-ENIG exposed outdoors for 3 months.

3.2. EIS analysis

The EIS data of PCB samples exposed outdoors for different periods is shown in Fig. 3 as a Nyquist diagram, a Bode phase diagram and a Bode modulus diagram. Except for the EIS data of PCB-Cu exposed for 6 months, all the other impedance data were fitted by an equivalent circuit shown in Fig. 4(a), where R_s is the solution resistance, R_p and Q_p (constant phase angle element) represent the resistance and capacitance behavior, respectively, of the protective layer of oxide film and/or corrosion product, Q_{dl} is the double-layer capacitance and R_{ct} is the charge transfer resistance.

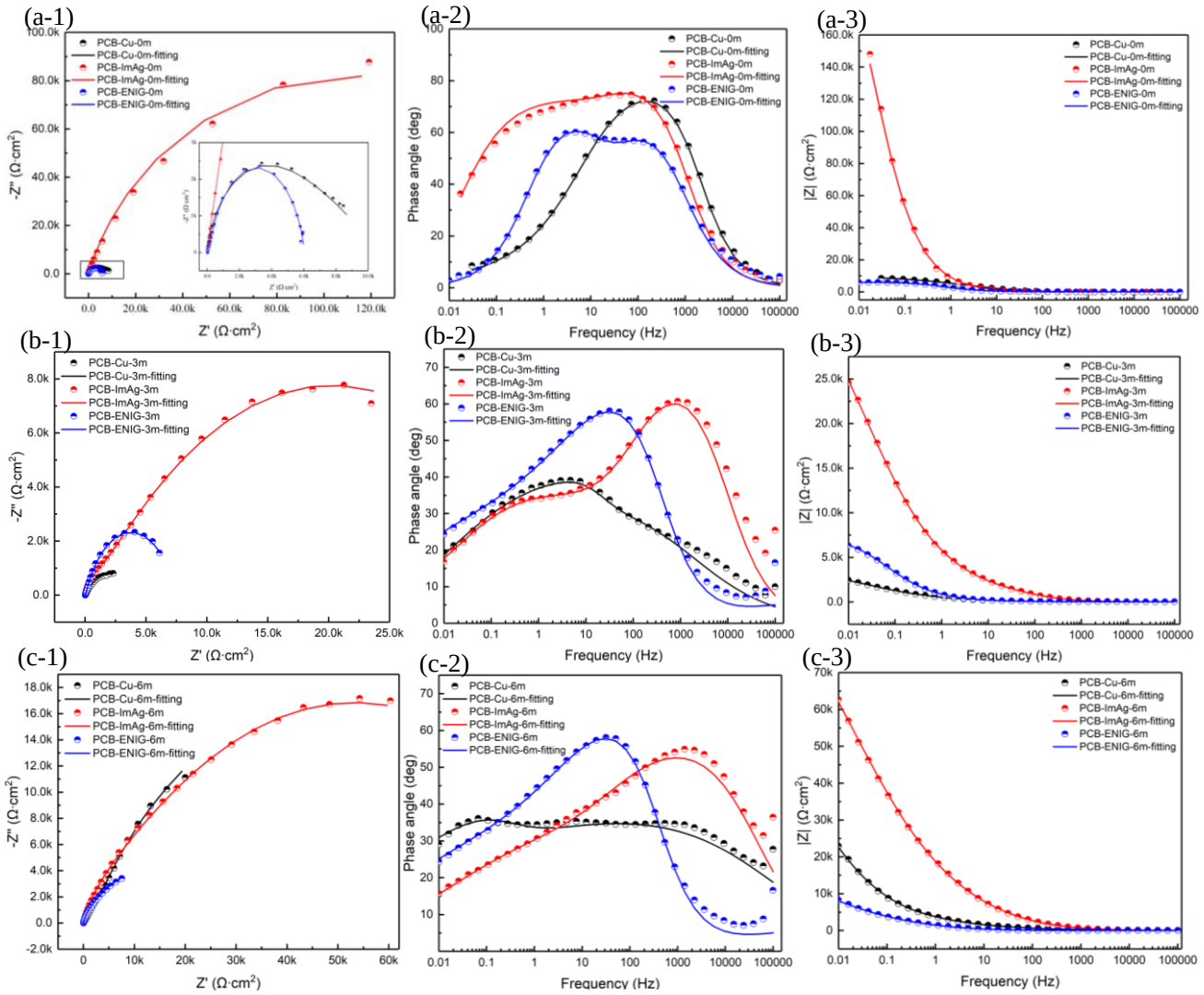

Figure 3. EIS data of PCBs exposed outdoors for (a) 0 m (b) 3 m and (c) 6 m. (1) Nyquist diagram, (2) Bode phase diagram and (3) Bode modulus diagram.

The fitted parameters are listed in Table 2. For PCB-Cu, since it was reported that long-term exposure would lead to the formation of corrosion products of a two-layered structure, with an inner dense oxide film of copper and an outer layer of loose copper salts25 [25], the EIS data of PCB-Cu exposed for 6 months was fitted using the equivalent circuit in Fig. 4(b), where Q_1 and R_1 represent the

resistance and capacitance of outer corrosion products, respectively, while Q_2 and R_2 represent the corresponding parameters of the inner corrosion products, and C_{dl} represents the double-layer capacitance. The meaning of other elements was the same as in Fig. 4(a). The corresponding fitted results are shown in Table 3

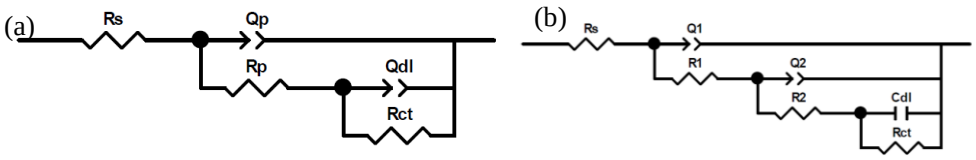

Figure 4. Equivalent electrical circuit for PCBs exposed outdoors. (a) Common, (b) PCB-Cu exposed for 6 months.

Table 2. Fitting equivalent circuit parameters for the impedance spectra of PCBs exposed outdoors for different periods except PCB-Cu exposed for 6 months.

Time(m)	Material	R_s ($\Omega\cdot cm^2$)	Q_p-Y_0 ($\Omega^{-1}\cdot cm^{-2}\cdot s^{-n}$)	Q_p-n	R_p ($\Omega\cdot cm^2$)	Q_{dl}-Y_0 (Ω^{-1} cm^{-2} s^{-n})	Q_{dl}-n	R_{ct} ($k\Omega\cdot cm^2$)
0	PCB-Cu	20.72	4.198E-5	0.3612	2.513	5.781E-6	0.9360	10.58
0	PCB-ImAg	20.74	1.347E-5	0.9204	3293	1.258E-5	0.6920	229.8
0	PCB-ENIG	19.23	3.592E-5	0.8387	527.4	3.458E-5	0.8537	5.500
3	PCB-Cu	21.91	7.280E-4	0.4615	548.7	2.016E-5	0.9375	3.561
3	PCB-ImAg	28.02	4.316E-6	0.8209	1372	7.248E-5	0.4766	38.53
3	PCB-ENIG	22.85	9.852E-5	0.8058	138.0	2.170E-4	0.6720	7.381
6	PCB-ImAg	54.51	3.991E-6	0.6705	6359	2.367E-5	0.3788	101.2
6	PCB-ENIG	13.88	2.492E-4	0.3717	14.71	4.224E-5	0.8609	26.79

Table 3. Fitting equivalent circuit parameters for the impedance spectra of PCB-Cu exposed outdoors for 6 months.

R_s ($\Omega\cdot cm^2$)	Q_1-Y_0 ($\Omega^{-1}\cdot cm^{-2}\cdot s^{-n}$)	Q_1-n	R_1 ($\Omega\cdot cm^2$)	Q_2-Y_0 (Ω^{-1} cm^{-2} s^{-n})	Q_2-n	R_1 ($\Omega\cdot cm^2$)	C_{dl} ($\mu F\cdot cm^{-2}$)	R_{ct} ($\Omega\cdot cm^2$)
35.78	1.046E-4	0.4188	1.787E4	3.748E-5	0.7382	7.598E4	1.763E-2	38.23

Two time constants were observed in Fig. 3 for PCBs exposed for different periods, except PCB-Cu exposed for 6 months, which correspond to the product layer and the double layer. For PCB-Cu exposed for 6 months, there were three time constants; they correspond to outer corrosion products, inner oxide film and double layer. The difference above showed that the corrosion process of PCB-ImAg and PCB-ENIG during exposure experiments remained unchanged and similar, but the corrosion process for PCB-Cu changed, which was probably related to the structural change of the corrosion products from a single oxide layer to a double layer containing inner and outer corrosion products. From Fig. 3(3), during the total exposure stage, the impedance of PCB-ImAg was much higher than that of PCB-Cu and PCB-ENIG, which indicated that the PCB-ImAg had excellent corrosion resistance.

As previously reported, capacitive loops can reflect the corrosion resistance of metal, and the capacitive loops are related to the R_{ct} [26]. Typically, the R_{ct} can reflect the size of the interfacial reaction resistance and has often been used to compare the corrosion rate, where a higher R_{ct} value represents a lower corrosion rate and vice versa [27]. The change trend of R_{ct} during exposure periods is shown in Fig. 5. It can be seen that the R_{ct} of PCB-ImAg decreased at an early stage; a severe exposure condition and weak protective layer promoted the corrosion of PCB-ImAg. With increasing exposure time, the corrosion products accumulated gradually and the products layer became denser, so the protective effect was enhanced and R_{ct} showed an increase. During the exposure periods, the corrosion product layer of PCB-ENIG became increasingly dense, so the R_{ct} of PCB-ENIG increased constantly, but its R_{ct} was always lower than that of PCB-ImAg, revealing that the corrosion resistance of PCB-ENIG was weaker than that of PCB-ImAg. Previous research had reported that the resistance of a silver coating for Cl^- was strong and that PCB-ImAg had high sensitivity to SO_2 and H_2S [9, 24]; however, in the tropical marine atmosphere environment of this paper, the main corrosive substance was Cl^- rather than SO_2 or H_2S. Thus, PCB-ImAg had a stronger corrosion resistance and a lower corrosion rate. For PCB-Cu, its R_{ct} constantly decreased as exposure time increased to 6 months, which may be attributed to the lack of a protective coating. Although corrosion products were formed, the corrosion product layer was loose and porous and could even shed from the substrate, as shown in Fig. 1 (a-3), so the corrosion products of PCB-Cu could not provide effective protection for the copper substrate, and the corrosion rate of PCB-Cu increased gradually.

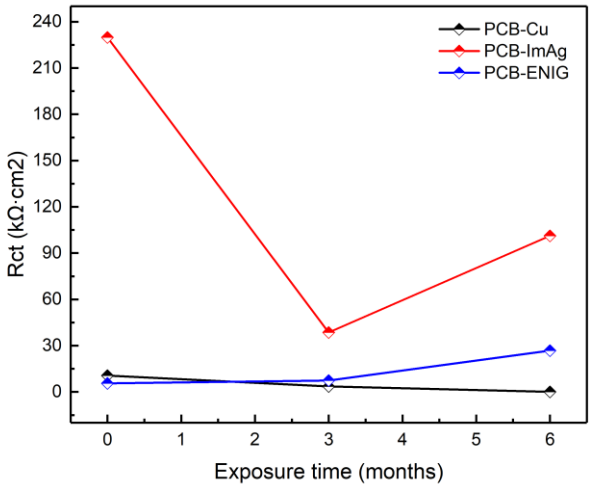

Figure 5. The relationship between R_{ct} and exposure time.

In general, during the exposure experiments, the corrosion rate of PCB-ImAg was the lowest, and it showed excellent corrosion resistance, followed by PCB-ENIG, while the corrosion rate of PCB-Cu was the highest, and the corresponding corrosion resistance was poor, which was in good agreement with the SEM morphology.

3.3. Corrosion mechanism

Based on the experimental results above and previous studies, a corrosion mechanism of PCBs in a tropical marine atmosphere is proposed, and Fig. 6 shows the corrosion scheme of different surface-treated PCBs.

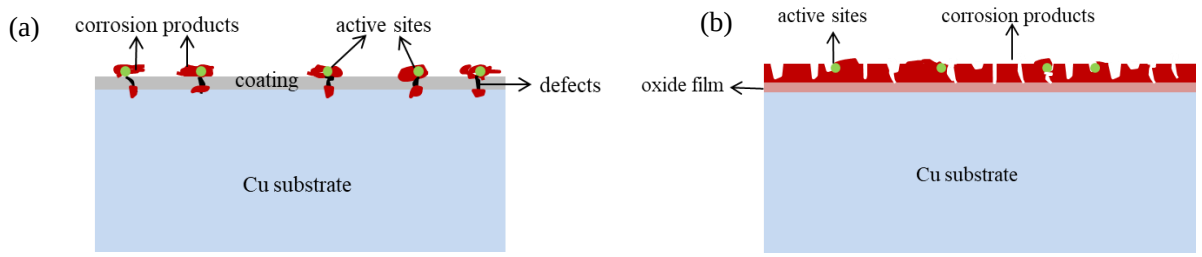

Figure 6. Scheme of corrosion mechanism for (a) PCB-ImAg and PCB-ENIG, (b) PCB-Cu.

As for PCB-ImAg and PCB-ENIG, although the coating covering the copper substrate could keep the copper substrate away from the outer corrosive environment, some defects, such as cracks and pores, were unavoidably generated in the manufacturing process and would weaken the protection effects of the coating [28]. Additionally, corrosion problems related with these microdefects have been reported [11, 29, 30]. According to these reports, the corrosion of copper with noble metal layers was ascribed to the formation of a localized corrosion cell, with the copper substrate serving as anode and gold or silver serving as cathode, and defects in the coating layers served as a pathway between the surface coating layer and the copper substrate for electrical conduction. The corrosion mechanism above was proposed under a corrosive condition mainly containing a contaminating gas such as reduced sulfur gas or sulfur oxides; however, in the tropical marine atmosphere environment of this paper, the main factors related to corrosion were the deposition of salt particles and attachment of microorganisms. There were many salt particles, mold spores and dust particles scattered on the samples' surfaces, leading vapor to condense or adsorb and promoting the formation of a thin electrolyte layer at these points. The corrosive electrolyte liquid, including chloride ions and metabolites of microorganisms, would pass through the transport pathways of defects and reach the copper substrate, and the corrosive substances would directly attack the copper substrate. Further, the corrosion of Cu was accelerated under the influence of the localized corrosion cell. In particular, the cathode of the protective layer had a much larger area than the anode of the copper exposed to the electrolyte, so the corrosion current density of anodic Cu would be high. Moreover, the corrosion products formed in the micropores or microcracks would migrate to the surface of the metal. With increasing time, the corrosion products accumulated and became dense, which could prevent the corrosive medium from reaching the copper substrate and inhibit further corrosion, which was consistent with the increase of R_{ct} value above.

Without the protective effect of a coating, PCB-Cu easily suffered from surface oxidation. In particular, the settlements of many salt particles and mold spores had low potential and would be preferentially corroded, which was previously reported [4], so there was an oxide film covering on the copper substrate at an early stage of exposure. With increasing time, many salt particles and some

contaminants would participate in the corrosion reaction at the active sites, and the corrosion products of copper salts would be formed and gradually accumulate. It was reported that the corrosion products of Cu in an atmosphere environment containing Cl^- also contained $Cu_2(OH)_3Cl$, $Cu_2(OH)_2CO_3$, etc., and these copper salts were loose and porous [25, 31, 32]. After long-term exposure, a double layer of corrosion products formed, as shown in Fig. 6(b), and this double-layer structure has been previously reported [4, 25]. Therefore, the EIS results of PCB-Cu exposed for 6 months had three time constants rather than two time constants. The corrosion products layer of Cu salts was loose and porous, and the inner oxide film was not dense enough to protect the substrate, so the corrosive medium could continue to reach the copper substrate, and the corrosion rate increased constantly, which is in good agreement with the decreasing R_{ct} of PCB-Cu.

4. CONCLUSIONS

The research results for the corrosion behavior of PCBs exposed in a tropical marine atmosphere environment were as follows:

1. PCB-ImAg had excellent corrosion resistance in the tropical marine atmosphere. PCB-ImAg had strong resistance to Cl^- present in the tropical marine atmosphere, there were only several spores scattered on the surface of PCB-ImAg, and no obvious corrosion characteristics were observed on its surface. Additionally, the EIS analysis demonstrated that PCB-ImAg had a high impedance and a low corrosion rate. PCB-ENIG was covered with dense corrosion products, and it had poor biocompatibility and was detrimental to the growth of molds. PCB-Cu was corroded significantly, and obvious shedding of the surface corrosion products was observed. EIS data verified that the corrosion rate of PCB-Cu increased constantly during the exposure periods.

2. A corresponding corrosion mechanism of PCBs was proposed. All the corrosion occurred at active sites where salt particles, mold spores and dust particles were scattered. When the copper substrate was covered by a coating, the defects of the coating served as pathways for the corrosive electrolyte liquid, and the copper substrate was corroded; a localized corrosion cell accelerated the corrosion. For PCB-Cu, long-term exposure would lead to the formation of a double-layer structure with an inner oxide film and outer loose corrosion products, and the corrosion products could not provide effective protection for the copper substrate, and thus PCB-Cu was constantly corroded.

ACKNOWLEGEMENTS
This work was supported by the National Natural Science Foundation of China (Nos. 51671027 and 51771027) and the National Environmental Corrosion Platform (NECP, 2005DKA10400).

References

1. A. Skwarek, K. Witek and J. Ratajczak, *Microelectron. Reliab*., 49 (2009) 569.
2. R. Ambat, P. Møller, *Corros. Sci*., 49 (2007) 2866.
3. W. Gen, X. Chen, A. Hu and M. Li, *Microelectron. Reliab*., 51 (2011) 866.
4. P. Yi, C. Dong, K. Xiao and X. Li, *Appl. Surf. Sci*., 399 (2017) 608.
5. M. Yang and Z. Y. Wang. , *Eq. Environ. Eng*., 3 (2006) 38.
6. K. P. FitzGerald, J. Nairn, G. Skennerton and A. Atrens, *Corros. Sci*., 48 (2006) 2480.
7. J. Zhang, Z. Liu, G. Han, S. Chen and Z. Chen*, Appl. Surf. Sci*., 389 (2016) 601.
8. W. Wang, A. Choubey, M. H. Azarian and M. Pecht*, J. Electron. Mater*., 38 (2009) 815.
9. L. Yan, K. Xiao, P. Yi, C. Dong, J. Wu, Z. Bai, C. Mao, L. Jiang and X. Li, *Mater. Des*.,115 (2017) 404.
10. B. K. Kim, S. J. Lee, J. Y. Kim, K. Y. Ji, Y. J. Yoon, M. Y. Kim, S. H. Park and J. S. Yoo, *J. Electron. Mater.*, 4 (2008) 527.
11. P. Yi, K. Xiao, K. Ding, C. Dong and X. Li, *Mater. Res. Bull*., 91 (2017) 179.
12. K. Ding, K. Xiao, C. Dong, S. Zou, P. Yi, and X. Li, *J. Electron. Mater*., 44 (2015)4405.
13. G. A. El-Mahdy, A. Nishikata and T. Tsuru, *Corros. Sci*., 42(2000) 1509.
14. H. Huang, X. Guo, G. Zhang and Z. Dong, *Corros. Sci.,* 53 (2011) 1700.
15. H. Huang, Z. Dong, Z. Chen and X. Guo, *Corros. Sci*., 53 (2011) 1230.
16. Z. Y. Chen, S. Zakipour, D. Persson and C. Leygraf, *Corrosion,* 61 (2005) 1022.
17. S. Zou, X. Li, C. Dong, K. Ding and K. Xiao, *Electrochim. Acta*, 114 (2013) 363.
18. C. A. C. Sequeira, *Brit. Corros. J*., 30 (1995) 137.
19. S. Zou, X. Li, C. Dong, H. Li and K. Xiao, *Acta Metall. Sin*., 48 (2012) 687.
20. S. Zou, K. Xiao, C. Dong, H. Li and X. Li, *Sci. Technol. Rev*., 30 (2012) 21.
21. S. Feliu, M. Morcillo and S. F. Jr, *Corros. Sci*., 34 (1993) 415.
22. P. Yi, K. Xiao, K. Ding, G. Li, C. Dong, and X. Li, *Trans. Nonferrous Met. Soc. China*, 26(2016) 1146.
23. N. Li, B. Li and J. Hu, *Sci. Technol. Rev.,* 28 (2010) 41.
24. P. Mazurkiewicz, Proceedings of the 32nd International Symposium for Testing and Failure Analysis, Texas, USA (2006).
25. H. Strandberg, *Atmos. Environ*., 32 (1998) 3511.
26. L. Chen, P. Zhang, Q. Xiong, P. Zhao, J. Xiong and Y. Zhou, *Int. J. Electrochem. Sci*., 14 (2019) 919.
27. B.A. Abd-El-Nabey, A. M. Abdel-Gaber, M. El. S. Ali, E. Khamis and S. El-Housseiny, *Int. J. Electrochem. Sci*., 8 (2013) 5851.
28. R. Ramanauskas, A. Selskis, J. Juodkazyte, and V. Jasulaitiene, *Circuit World*, 39 (2013) 124.
29. Martens R. and Pecht M. G., *IEEE T. Adv. Packaging*, 23 (2002) 561.
30. K. Hannigan, M. Reid, M. N. Collins, E. Dalton, C. Xu, B. Wright, K. Demirkan, R. L. Opila, W. D. Reents Jr, J. P. Franey, D. A. Fleming and J. Punch, *J. Electron. Mater*., 41 (2012) 611.
31. G. Kear, B. D. Barker and F. C.Walsh, *Corros. Sci.,* 46 (2004) 109.
32. A. R. Mendoza, F. Corvo, A. Gómez and J. Gómez, *Corros. Sci*., 46 (2004) 1189.